

Orbital-Controlled Superconductivity in f -Electron Systems

Katsunori KUBO and Takashi HOTTA

Advanced Science Research Center, Japan Atomic Energy Agency, Tokai, Ibaraki 319-1195

(Received May 16, 2006; accepted June 8, 2006; published July 25, 2006)

We propose a concept of superconductivity controlled by orbital degree of freedom taking $CeMIn_5$ ($M = Co, Rh, \text{ and } Ir$) as typical examples. A microscopic multiorbital model for $CeMIn_5$ is analyzed by fluctuation exchange approximation. Even though the Fermi-surface structure is unchanged, the ground state is found to change significantly among paramagnetic, antiferromagnetic, and d -wave superconducting phases, depending on the dominant orbital component in the band near the Fermi energy. We show that our picture naturally explains the different low-temperature properties of $CeMIn_5$ by carefully analyzing the crystalline electric field states.

KEYWORDS: crystalline electric field, heavy-fermion superconductor, fluctuation exchange approximation, thermal expansion

Since the discovery of heavy-fermion superconductivity in $CeCu_2Si_2$,¹ it has been one of the central issues in the research field of condensed matter physics to unveil unconventional superconductivity in strongly correlated electron systems. In particular, it is important to determine a key parameter for controlling the appearance of superconductivity. Among heavy-fermion superconductors, $CeMIn_5$ ($M = Co, Rh, \text{ and } Ir$) have potential for systematic understanding of the mechanism and control parameter of superconductivity, since various ordered phases have been found in the same crystal structure. At ambient pressure, a relatively high superconducting transition temperature $T_c = 2.3$ K has been reported for $CeCoIn_5$,² whereas $T_c = 0.4$ K for $CeIrIn_5$.³ $CeRhIn_5$ is an antiferromagnet with a Néel temperature $T_N = 3.8$ K at ambient pressure, but it becomes superconducting with $T_c \simeq 2$ K at pressure $p \gtrsim 1.6$ GPa.⁴

The observed power-law temperature dependences of specific heat,^{2,5,6} thermal conductivity,⁵ and spin-lattice relaxation rate⁷⁻¹⁰ suggest the presence of line nodes in the superconducting gap function. In addition, the fourfold magnetic-field angular-dependences of thermal conductivity¹¹ and specific heat¹² clearly indicate d -wave superconductivity for $CeCoIn_5$. The existence of antiferromagnetism in $CeRhIn_5$ at ambient pressure is also consistent with d -wave superconductivity induced by antiferromagnetic fluctuations.

Concerning the control parameter of superconductivity, one may first consider carrier density, as in the case of high- T_c cuprates. In addition, Fermi-surface topology also plays a crucial role in the occurrence of superconductivity and the determination of the symmetry of the gap function. However, the carrier densities are essentially the same among $CeMIn_5$, because f -electron number per Ce ion is not changed by M . Furthermore, Fermi surfaces observed by de Haas-van Alphen experiments and band-structure calculations are similar among these compounds.¹³⁻¹⁸ Thus, neither the carrier density nor Fermi-surface topology is the main control parameter of superconductivity and antiferromagnetism in $CeMIn_5$.

Here, we point out another important ingredient, the

crystalline electric field (CEF) effect, in $CeMIn_5$. Immediately after the discovery of $CeMIn_5$, Takimoto *et al.* have stressed the importance of the CEF effect in controlling superconductivity,¹⁹ but only level splitting was taken into account. Note that CEF potential affects not only level splitting, but also the CEF ground-state wavefunction. In fact, recent inelastic neutron scattering experiments have revealed that level splittings are almost the same among $CeMIn_5$, whereas CEF wave-functions are quite different.²⁰ The importance of orbital states has been discussed for $Na_xCoO_2 \cdot yH_2O$,²¹ but the effects of the change in orbital states on superconductivity have not been studied systematically so far. It is conceptually important to clarify superconductivity controlled by orbital states.

In this Letter, we apply fluctuation exchange (FLEX) approximation to an f -electron model constructed on a square lattice for $CeMIn_5$. Such perturbative theories have been applied to one- f -orbital models for $CeMIn_5$.²²⁻²⁴ In this study, we focus on the effect of a CEF using a model including all the states with the total angular momentum $j = 5/2$, which are split into one Γ_6 and two Γ_7 doublets under a tetragonal CEF. Among them, the wave functions of Γ_7 states sensitively depend on CEF potential. We change the wave functions fixing level splittings, and determine both T_c and T_N within FLEX approximation. Even though the Fermi-surface structure does not change, the ground state changes depending on the Γ_7 wave-functions among the paramagnetic, antiferromagnetic, and d -wave superconducting states. We show that the obtained phase diagram is relevant to $CeMIn_5$.

Using the f -electron basis under a cubic CEF for convenience, we consider a three-orbital model based on a j - j coupling scheme on a square lattice given by

$$H = \sum_{\mathbf{r}, \mu, \tau, \tau', \sigma} t_{\tau\tau'}^\mu c_{\mathbf{r}\tau\sigma}^\dagger c_{\mathbf{r}+\mu\tau'\sigma} + U \sum_{\mathbf{r}\tau} n_{\mathbf{r}\tau\uparrow} n_{\mathbf{r}\tau\downarrow} + (U'/2) \sum_{\mathbf{r}, \tau \neq \tau'} n_{\mathbf{r}\tau} n_{\mathbf{r}\tau'} + H_{\text{CEF}}, \quad (1)$$

where $c_{\mathbf{r}\tau\sigma}$ is the annihilation operator of the f elec-

tron at site \mathbf{r} with the pseudospin σ and the orbital τ , $n_{\mathbf{r}\tau\sigma} = c_{\mathbf{r}\tau\sigma}^\dagger c_{\mathbf{r}\tau\sigma}$, and $n_{\mathbf{r}\tau} = \sum_{\sigma} n_{\mathbf{r}\tau\sigma}$. Note that σ ($=\uparrow$ and \downarrow) distinguishes two states in each Kramers doublet. On the other hand, τ is introduced to distinguish three kinds of Kramers doublets under a cubic CEF. Here, α and β denote two Γ_8 , while γ indicates Γ_7 . We use $t_{\tau\tau'}^\mu$ for the hopping amplitude between the τ' state at site $\mathbf{r} + \boldsymbol{\mu}$ and the τ state at \mathbf{r} , where $\boldsymbol{\mu}$ is a vector connecting nearest-neighbor sites. We consider the hopping through $(ff\sigma)$ bonding, given by $t_{\alpha\alpha}^{(a,0)} = t_{\alpha\alpha}^{(0,a)} = -\sqrt{3}t_{\alpha\beta}^{(a,0)} = -\sqrt{3}t_{\beta\alpha}^{(a,0)} = \sqrt{3}t_{\alpha\beta}^{(0,a)} = \sqrt{3}t_{\beta\alpha}^{(0,a)} = 3t_{\beta\beta}^{(a,0)} = 3t_{\beta\beta}^{(0,a)} = t$ and zero for the other cases,²⁵ where $t = 9(ff\sigma)/28$ and a is the lattice constant. The coupling constants U and U' denote intra- and inter-orbital Coulomb interactions, respectively. Note that we ignore the Hund's rule coupling, pair-hopping interaction, and the other interactions for simplicity. Then, owing to the symmetry requirement, we should set $U = U'$. We also note that t , U , and U' should be regarded as renormalized ones for heavy electrons.²⁶

The tetragonal CEF term H_{CEF} is given by

$$H_{\text{CEF}} = \sum_{\mathbf{r}} (B_2^0 O_{2\mathbf{r}}^0 + B_4^0 O_{4\mathbf{r}}^0 + B_4^4 O_{4\mathbf{r}}^4), \quad (2)$$

where B_m^n is the CEF parameter and $O_{m\mathbf{r}}^n$ is the Stevens operator equivalent at site \mathbf{r} .²⁷ We can rewrite eq. (2) with the basis of the cubic CEF eigenstates as $H_{\text{CEF}} = \sum_{\mathbf{r}, \sigma, \tau, \tau'} B_{\tau\tau'} c_{\mathbf{r}\tau\sigma}^\dagger c_{\mathbf{r}\tau'\sigma}$, where $B_{\tau\tau'}$ is given by an appropriate linear combination of B_m^n . From the diagonalization of H_{CEF} , we express the CEF parameters as $B_2^0 = [-4\Delta_{67} + \Delta_7(2\cos(2\theta) - \sqrt{5}\sin(2\theta))]/84$, $B_4^0 = [3\Delta_{67} + \Delta_7(2\cos(2\theta) - \sqrt{5}\sin(2\theta))]/1260$, and $B_4^4 = \sqrt{5}\Delta_7(\sqrt{5}\cos(2\theta) + 2\sin(2\theta))/360$, where Δ_{67} and Δ_7 determine CEF energy levels, while θ characterizes eigenstates under a CEF potential. Then, the CEF energy levels are $-\Delta_{67}/3 - \Delta_7/2$ for the $\Gamma_7^{(1)}$ states, $(c_{\mathbf{r}\gamma\sigma}^\dagger \cos\theta + c_{\mathbf{r}\alpha\sigma}^\dagger \sin\theta)|0\rangle$, $-\Delta_{67}/3 + \Delta_7/2$ for the $\Gamma_7^{(2)}$ states, $(-c_{\mathbf{r}\gamma\sigma}^\dagger \sin\theta + c_{\mathbf{r}\alpha\sigma}^\dagger \cos\theta)|0\rangle$, and $2\Delta_{67}/3$ for the Γ_6 states, $c_{\mathbf{r}\beta\sigma}^\dagger|0\rangle$, where $|0\rangle$ denotes vacuum.

Now we apply FLEX approximation, which has been extended for multiorbital models.²⁸⁻³¹ Since σ is a conserved quantity in the present model, the Green's function does not depend on σ and is represented by a 3×3 matrix. In a matrix form, the Dyson-Gorkov equation is given by $G(\mathbf{k}) = G^{(0)}(\mathbf{k}) + G^{(0)}(\mathbf{k})\Sigma(\mathbf{k})G(\mathbf{k})$, where $G(\mathbf{k})$ is the Green's function and $G^{(0)}(\mathbf{k})$ is the noninteracting Green's function. Here, we have introduced the abbreviation $\mathbf{k} = (\mathbf{k}, i\epsilon_n)$, where \mathbf{k} is the momentum and $\epsilon_n = (2n+1)\pi T$ is the fermion Matsubara frequency with an integer n and a temperature T . The self-energy is given by

$$\Sigma_{\tau_1\tau_2}(k) = \frac{T}{N} \sum_{q\tau_1'\tau_2'} V_{\tau_1\tau_1';\tau_2\tau_2'}(q) G_{\tau_1'\tau_2'}(k-q), \quad (3)$$

where N is the number of lattice sites, $q = (\mathbf{q}, i\omega_m)$, and $\omega_m = 2m\pi T$ is the boson Matsubara frequency. The fluctuation exchange interaction is given by $V(q) = \frac{3}{2}[U^s\chi^s(q)U^s - U^s\chi^{(0)}(q)U^s/2 + U^s] + \frac{1}{2}[U^c\chi^c(q)U^c - U^c\chi^{(0)}(q)U^c/2 - U^c]$. The matrices U^s and U^c are given by $U_{\tau\tau';\tau\tau}^s = U_{\tau\tau';\tau\tau}^c = U$, $U_{\tau\tau';\tau\tau'}^s = -U_{\tau\tau';\tau\tau'}^c = U'$,

and $U_{\tau\tau';\tau'\tau'}^c = 2U'$, where $\tau \neq \tau'$, and the other matrix elements are zero. The spin and charge parts of the susceptibility are given by $\chi^s(q) = \chi^{(0)}(q)[1 - U^s\chi^{(0)}(q)]^{-1}$ and $\chi^c(q) = \chi^{(0)}(q)[1 + U^c\chi^{(0)}(q)]^{-1}$, respectively, where $\chi_{\tau_1\tau_2;\tau_3\tau_4}^{(0)}(q) = -\frac{T}{N} \sum_{\mathbf{k}} G_{\tau_1\tau_3}(\mathbf{k}+q)G_{\tau_4\tau_2}(\mathbf{k})$.

In FLEX approximation without vertex corrections, the magnetic susceptibility is given by³²

$$\chi_\nu(q) = \frac{1}{2} \sum_{\substack{\tau_1-\tau_4 \\ \sigma_1-\sigma_4}} \chi_{\tau_1\tau_2;\tau_3\tau_4}^s(q) J_{\tau_2\sigma_2;\tau_1\sigma_1}^\nu J_{\tau_3\sigma_3;\tau_4\sigma_4}^\nu \sigma_{\sigma_1\sigma_2}^\nu \sigma_{\sigma_4\sigma_3}^\nu, \quad (4)$$

where $\nu = x, y, \text{ or } z$, $\boldsymbol{\sigma}$ are the Pauli matrices, and $J_{\tau_2\sigma_2;\tau_1\sigma_1}^\nu$ is the matrix element of the operator of the dipole moment. In this paper, we renormalize J^ν so that the sum of squares of eigenvalues is unity, for convenience. The linearized equation for the anomalous self-energy ϕ is expressed as

$$\phi_{\tau_1\tau_2}^\xi(k) = -\frac{T}{N} \sum_{k'\tau_1'\tau_2'} K_{\tau_1\tau_2;\tau_1'\tau_2'}^\xi(k, k') \phi_{\tau_1'\tau_2'}^\xi(k'), \quad (5)$$

where ξ denotes the pseudospin singlet (S) or triplet (T) pairing state and the kernel is given by $K_{\tau_1\tau_2;\tau_1'\tau_2'}^\xi(k, k') = \sum_{\tau_3\tau_4} V_{\tau_1\tau_3;\tau_4\tau_2}^\xi(k-k') G_{\tau_3\tau_1'}(k') G_{\tau_4\tau_2'}(-k')$. The effective pairing interactions are given by $V^S(q) = \frac{3}{2}[U^s\chi^s(q)U^s + U^s/2] - \frac{1}{2}[U^c\chi^c(q)U^c - U^c/2]$ and $V^T(q) = -\frac{1}{2}[U^s\chi^s(q)U^s + U^s/2] - \frac{1}{2}[U^c\chi^c(q)U^c - U^c/2]$. The transition temperature of superconductivity is given by the temperature where eq. (5) has a nontrivial solution.

In the following, we show results for a 32×32 lattice for $U = U' = 4t$, $\Delta_{67} = 1.5t$, and $\Delta_7 = t$. The results are not so sensitive to precise values of Δ_{67} and Δ_7 as long as they are in the order of t . In the calculation, we use 1024 Matsubara frequencies. The number of f electrons per site is fixed to be one, since we are considering Ce^{3+} ions. The present model with the CEF parameter θ is invariant for $\theta \rightarrow \theta + \pi$. In addition, when $U = U'$, the model is also invariant for $\theta \rightarrow -\theta$. Thus, it is enough to consider $0 \leq \theta \leq \pi/2$.

Figures 1(a)–1(c) show the magnetic susceptibility $\chi_\nu(\mathbf{q}) = \chi_\nu(\mathbf{q}, i\omega_m = 0)$ for $\theta = 0, \pi/4$, and $\pi/2$, respectively. It is observed that $\chi_\nu(\mathbf{q})$ strongly depends on θ . In the following, we explain this dependence from the viewpoint of itinerant and localized orbitals.

First, let us discuss the noninteracting susceptibility $\chi_\nu^{(0)}(\mathbf{q})$ [Figs. 1(d)–1(f)]. In Figs. 1(g)–1(l), we show noninteracting band structures and Fermi-surface curves. Even if θ is changed, the band that crosses the Fermi level E_F has similar dispersion at E_F , leading to an almost the same Fermi surface. Note, however, that in general, $\chi_\nu^{(0)}(\mathbf{q})$ depends on the band structure and is not determined solely by the Fermi surface structure (*e.g.*, nesting property), particularly for multiorbital systems. The nearly flat band composed mainly of the γ orbital locates near E_F for small θ ,³³ suggesting that electrons near E_F have nearly localized character.³⁴ Thus, $\chi_\nu^{(0)}(\mathbf{q})$ for $\theta = 0$ is almost flat in momentum space. For small θ , the magnitude of $\chi_\nu^{(0)}(\mathbf{q})$ is large, since $\chi_\nu^{(0)} \sim \rho_0$ at sufficiently low T , where ρ_0 is the density of states at E_F , and it becomes large when the localized character is strong.

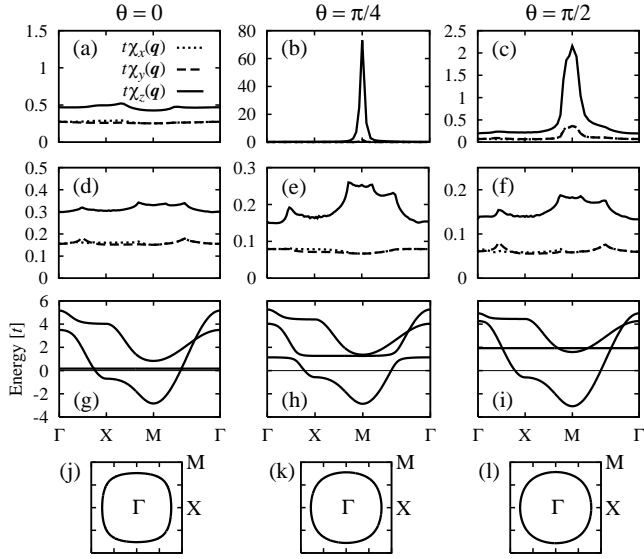


Fig. 1. (a)–(c) Magnetic susceptibility at $U = U' = 4t$ and $T = 0.02t$, for $\theta = 0, \pi/4$, and $\pi/2$, respectively. (d)–(f) Magnetic susceptibility at $U = U' = 0$ and $T = 0.02t$, for $\theta = 0, \pi/4$, and $\pi/2$, respectively. (g)–(i) Energy band structures at $U = U' = 0$ for $\theta = 0, \pi/4$, and $\pi/2$, respectively. The Fermi energy is set at zero (thin lines). (j)–(l) Fermi-surface curves at $U = U' = 0$ for $\theta = 0, \pi/4$, and $\pi/2$, respectively. The parameters are set at $\Delta_{67} = 1.5t$ and $\Delta_7 = t$.

With increasing θ , the localized character is weakened. Thus, $\chi_\nu^{(0)}(\mathbf{q})$ shows a structure in \mathbf{q} space and becomes smaller in magnitude. In particular, we observe a moderate enhancement around $\mathbf{q} = \mathbf{Q} \equiv (\pi/a, \pi/a)$ for $\theta = \pi/4$ and $\pi/2$.

Now, we consider the effect of on-site Coulomb interactions. We expect that the Fermi surface is not markedly changed by the Coulomb interaction. First, note that the on-site Coulomb interactions suppress the \mathbf{q} -independent part of $\chi_\nu^{(0)}(\mathbf{q})$ due to the correlation effect beyond random phase approximation (RPA). Thus, for small θ , $\chi_\nu(\mathbf{q})$ is totally suppressed in comparison with that of RPA. For larger θ , the structure in $\chi_\nu^{(0)}(\mathbf{q})$ grows to a peak at $\mathbf{q} = \mathbf{Q}$ in $\chi_\nu(\mathbf{q})$. On the other hand, such a peak becomes high and sharp, when the Coulomb interactions are effectively strong as for almost localized electrons at small θ . Thus, due to the combination of the band structure and the effect of the Coulomb interactions, $\chi_\nu(\mathbf{q})$ is large for a moderate value of $\theta \simeq \pi/4$ with a peak at $\mathbf{q} = \mathbf{Q}$.

In Fig. 2, we show a T - θ phase diagram. In this paper, we define T_N as a temperature at which $\chi_z(\mathbf{Q})$ reaches $100/t$. Note that the susceptibility does not become as large as $100/t$ for the other components χ_x and χ_y , or for \mathbf{q} other than \mathbf{Q} . The overall structure in Fig. 2 is consistent with the θ dependence of the magnetic property. Note that a d -wave singlet superconducting state with B_{1g} symmetry appears at $\theta \gtrsim 0.29\pi$ next to the antiferromagnetic phase. On the other side of the antiferromagnetic phase, T_c is very low,³⁵ even if the superconducting phase exists. This is consistent with the fact that the energy scale in the small- θ region becomes small owing to the strong localized character of electrons.

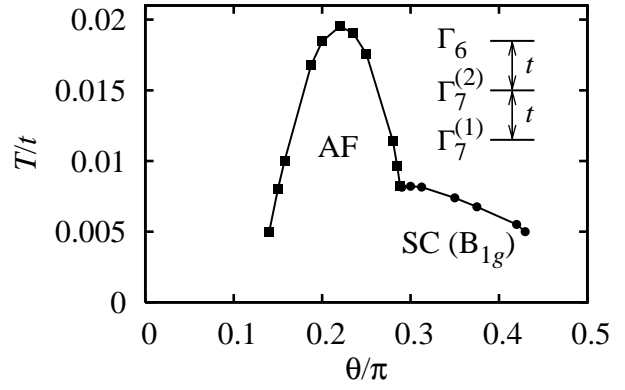


Fig. 2. Phase diagram for $U = U' = 4t$, $\Delta_{67} = 1.5t$, and $\Delta_7 = t$. Solid squares denote antiferromagnetic (AF) transition temperatures, while solid circles denote superconducting (SC) transition temperatures with B_{1g} symmetry.

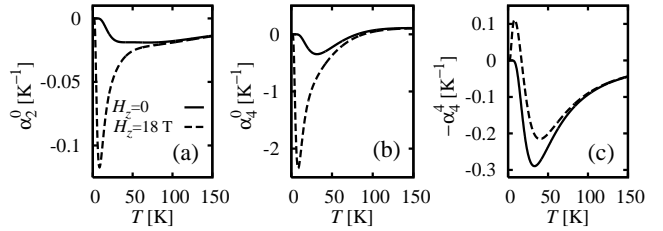


Fig. 3. Temperature dependences of (a) α_2^0 , (b) α_4^0 , and (c) $-\alpha_4^4$ for single ion under CEF potential deduced from neutron scattering experiment on CeRhIn_5 .²⁰ Solid curves denote the values without a magnetic field and dashed curves denote those in a magnetic field $H_z = 18$ T along the c -axis.

Now we discuss possible relevance of our results to CeMIn_5 . For this purpose, it is necessary to estimate θ for each material. Among the CEF parameters, the sign of B_4^4 is quite important, since the orbital state is markedly affected by the sign. Although inelastic neutron scattering is a powerful method of determining CEF energy levels, the sign of B_4^4 cannot be determined solely by neutron scattering experiment. Thus, we should perform CEF analysis of a quantity sensitive to $\langle O_4^4 \rangle$, where $\langle \dots \rangle$ denotes the expectation value in terms of H_{CEF} . Since the mode of charge distribution corresponding to finite $\langle O_4^4 \rangle$ couples to the lattice, thermal expansion is a good quantity for determining the sign of B_4^4 . Thermal expansion has been measured for CeMIn_5 , but the analysis focused only on the second-order term $\langle O_2^0 \rangle$.^{36–40} It is necessary to include fourth-order terms to analyze thermal expansion, as in the case of cubic systems.⁴¹

Figures 3(a)–3(c) show the temperature dependence of $\alpha_2^0 \equiv d\langle O_2^0 \rangle/dT$, $\alpha_4^0 \equiv d\langle O_4^0 \rangle/dT$, and $\alpha_4^4 \equiv d\langle O_4^4 \rangle/dT$, respectively, for the CEF parameters deduced from the neutron scattering experiment for CeRhIn_5 ,²⁰ assuming $B_4^4 > 0$. A thermal expansion coefficient is given by a linear combination of α_2^0 , α_4^0 , and α_4^4 . For $B_4^4 < 0$, α_4^4 changes its sign, whereas α_2^0 and α_4^0 do not. Although we do not show the calculated results for CeCoIn_5 and CeIrIn_5 , it has been found that the overall features are similar among CeMIn_5 . Figures 3(a)–3(c) show that the

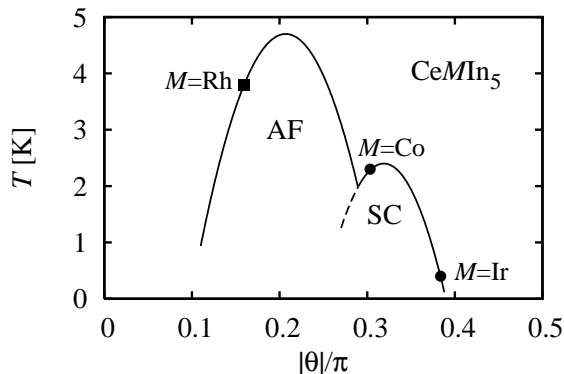


Fig. 4. Schematic phase diagram for $CeMIn_5$. Solid square and circles denote T_N and T_c , respectively. Curves are guides for the eyes. See the main text for the values of θ .

magnetic-field effect on α_2^0 and α_4^0 is strong, but weak on α_4^4 . From the experimental results,^{38,39} the magnetic-field effect on the thermal expansion coefficient α_c along the c -axis for $CeRhIn_5$ is not so significant as that observed in Figs. 3(a) and 3(b). Rather it looks similar to that in Fig. 3(c). Moreover, the minimum with a negative value in $-\alpha_4^4$ shifts toward higher temperatures under a magnetic field, as is experimentally observed in α_c of $CeRhIn_5$. Thus, we highly expect that α_c in $CeMIn_5$ is mainly determined by α_4^4 . For $CeCoIn_5$ and $CeIrIn_5$, α_c is always positive at the temperatures reported,^{36,37} in sharp contrast to that for $CeRhIn_5$. These observations indicate that the signs of B_4^4 for $CeCoIn_5$ and $CeIrIn_5$ are the same, but are different from that for $CeRhIn_5$.

For further quantitative analysis, it is necessary to have more precise knowledge on elastic constants and/or magnetoelastic coupling, but it is out of the scope of this paper. Rather, we phenomenologically assume $B_4^4 > 0$ for $CeRhIn_5$. Then, B_4^4 is negative for $CeCoIn_5$ and $CeIrIn_5$. By using the CEF parameters deduced from the neutron scattering experiment,²⁰ we obtain $\theta = 0.16\pi$ for $CeRhIn_5$, $\theta = -0.30\pi$ for $CeCoIn_5$, and $\theta = -0.38\pi$ for $CeIrIn_5$. In Fig. 4, we show a schematic phase diagram using these values of θ and experimental results for T_c and T_N . This is consistent with the theoretically determined phase diagram in Fig. 2. In addition, $CeRhIn_5$ locates in a small- θ region, indicating that f electrons in $CeRhIn_5$ have a relatively localized character, as is suggested from de Haas-van Alphen experiment.¹⁷ Thus, we conclude that the characteristics of $CeMIn_5$ can be captured by our model and that the main control parameter of antiferromagnetism and superconductivity for $CeMIn_5$ is θ which describes CEF wave-functions. To confirm this, it is important to experimentally determine CEF parameters for $CeMIn_5$ under pressure.

In summary, we have studied the f -electron model including all the states with $j = 5/2$ by FLEX approximation. We have found three kinds of ground state, i.e., paramagnetic, antiferromagnetic, and d -wave superconducting states, by changing the CEF wave-functions characterized by the parameter θ , even if we fix level splitting. Such phase change originating from the difference in character of f -electron orbitals explains well the

difference in $CeMIn_5$. This finding shows that, in general, orbital character can be a control parameter of superconductivity, in addition to Fermi surface topology and carrier density. The orbital-controlled superconductivity would be realized also in other f -electron materials with active orbital degrees of freedom, and the present study will provide an important step toward the investigation of such exotic superconductivity.

We are grateful to T. Takeuchi for sending us unpublished data of $CeCoIn_5$. We also thank T. Takimoto for useful discussions on FLEX calculation. The authors are supported by a Grant-in-Aid for Scientific Research in Priority Area ‘‘Skutterudites’’ from the Ministry of Education, Culture, Sports, Science, and Technology of Japan. K. K. is also supported by the REIMEI Research Resources of Japan Atomic Energy Agency and by a Grant-in-Aid for Young Scientists from the Ministry of Education, Culture, Sports, Science, and Technology of Japan. T. H. is also supported by a Grant-in-Aid for Scientific Research from the Japan Society for the Promotion of Science.

- 1) F. Steglich, J. Aarts, C. D. Bredl, W. Lieke, D. Meschede, W. Franz and H. Schäfer: Phys. Rev. Lett. **43** (1979) 1892.
- 2) C. Petrovic, P. G. Pagliuso, M. F. Hundley, R. Movshovich, J. L. Sarrao, J. D. Thompson, Z. Fisk and P. Monthoux: J. Phys.: Condens. Matter **13** (2001) L337.
- 3) C. Petrovic, R. Movshovich, M. Jaime, P. G. Pagliuso, M. F. Hundley, J. L. Sarrao, Z. Fisk and J. D. Thompson: Europhys. Lett. **53** (2001) 354.
- 4) H. Hegger, C. Petrovic, E. G. Moshopoulou, M. F. Hundley, J. L. Sarrao, Z. Fisk and J. D. Thompson: Phys. Rev. Lett. **84** (2000) 4986.
- 5) R. Movshovich, M. Jaime, J. D. Thompson, C. Petrovic, Z. Fisk, P. G. Pagliuso and J. L. Sarrao: Phys. Rev. Lett. **86** (2001) 5152.
- 6) R. A. Fisher, F. Bouquet, N. E. Phillips, M. F. Hundley, P. G. Pagliuso, J. L. Sarrao, Z. Fisk and J. D. Thompson: Phys. Rev. B **65** (2002) 224509.
- 7) Y. Kohori, Y. Yamato, Y. Iwamoto and T. Kohara: Eur. Phys. J. B **18** (2000) 601.
- 8) G.-q. Zheng, K. Tanabe, T. Mito, S. Kawasaki, Y. Kitaoka, D. Aoki, Y. Haga and Y. Onuki: Phys. Rev. Lett. **86** (2001) 4664.
- 9) Y. Kohori, Y. Yamato, Y. Iwamoto, T. Kohara, E. D. Bauer, M. B. Maple and J. L. Sarrao: Phys. Rev. B **64** (2001) 134526.
- 10) T. Mito, S. Kawasaki, G.-q. Zheng, Y. Kawasaki, K. Ishida, Y. Kitaoka, D. Aoki, Y. Haga and Y. Onuki: Phys. Rev. B **63** (2001) 220507(R).
- 11) K. Izawa, H. Yamaguchi, Y. Matsuda, H. Shishido, R. Settai and Y. Onuki: Phys. Rev. Lett. **87** (2001) 057002.
- 12) H. Aoki, T. Sakakibara, H. Shishido, R. Settai, Y. Onuki, P. Miranović and K. Machida: J. Phys.: Condens. Matter **16** (2004) L13.
- 13) A. L. Cornelius, A. J. Arko, J. L. Sarrao, M. F. Hundley and Z. Fisk: Phys. Rev. B **62** (2000) 14181.
- 14) Y. Haga, Y. Inada, H. Harima, K. Oikawa, M. Murakawa, H. Nakawaki, Y. Tokiwa, D. Aoki, H. Shishido, S. Ikeda, N. Watanabe and Y. Onuki: Phys. Rev. B **63** (2001) 060503(R).
- 15) D. Hall, E. C. Palm, T. P. Murphy, S. W. Tozer, C. Petrovic, E. Miller-Ricci, L. Peabody, C. Q. H. Li, U. Alver, R. G. Goodrich, J. L. Sarrao, P. G. Pagliuso, J. M. Wills and Z. Fisk: Phys. Rev. B **64** (2001) 064506.
- 16) R. Settai, H. Shishido, S. Ikeda, Y. Murakawa, M. Nakashima, D. Aoki, Y. Haga, H. Harima and Y. Onuki: J. Phys.: Condens. Matter **13** (2001) L627.
- 17) H. Shishido, R. Settai, D. Aoki, S. Ikeda, H. Nakawaki, N. Nakamura, T. Iizuka, Y. Inada, K. Sugiyama, T. Takeuchi,

- K. Kindo, T. C. Kobayashi, Y. Haga, H. Harima, Y. Aoki, T. Namiki, H. Sato and Y. Ōnuki: J. Phys. Soc. Jpn. **71** (2002) 162.
- 18) T. Maehira, T. Hotta, K. Ueda and A. Hasegawa: J. Phys. Soc. Jpn. **72** (2003) 854.
- 19) T. Takimoto, T. Hotta, T. Maehira and K. Ueda: J. Phys.: Condens. Matter **14** (2002) L369.
- 20) A. D. Christianson, E. D. Bauer, J. M. Lawrence, P. S. Riseborough, N. O. Moreno, P. G. Pagliuso, J. L. Sarrao, J. D. Thompson, E. A. Goremychkin, F. R. Hehlen and R. J. McQueeney: Phys. Rev. B **70** (2004) 134505.
- 21) Y. Yanase, M. Mochizuki and M. Ogata: J. Phys. Soc. Jpn. **74** (2005) 430.
- 22) Y. Nisikawa, H. Ikeda and K. Yamada: J. Phys. Soc. Jpn. **71** (2002) 1140.
- 23) H. Ikeda, Y. Nishikawa and K. Yamada: J. Phys.: Condens. Matter **15** (2003) S2241.
- 24) K. Tanaka, H. Ikeda and K. Yamada: J. Phys. Soc. Jpn. **73** (2004) 1285.
- 25) T. Hotta and K. Ueda: Phys. Rev. B **67** (2003) 104518.
- 26) Y. Yanase, T. Jujo, T. Nomura, H. Ikeda, T. Hotta and K. Yamada: Phys. Rep. **387** (2003) 1.
- 27) M. T. Hutchings: Solid State Phys. **16** (1964) 227.
- 28) T. Takimoto, T. Hotta and K. Ueda: Phys. Rev. B **69** (2004) 104504.
- 29) M. Mochizuki, Y. Yanase and M. Ogata: Phys. Rev. Lett. **94** (2005) 147005.
- 30) M. Mochizuki, Y. Yanase and M. Ogata: J. Phys. Soc. Jpn. **74** (2005) 1670.
- 31) K. Yada and H. Kontani: J. Phys. Soc. Jpn. **74** (2005) 2161.
- 32) K. Kubo and T. Hotta: cond-mat/0512647.
- 33) For $\theta = 0$, the CEF ground state is described purely by the γ orbital, but a band composed of other orbitals has lower energy at some wave-numbers due to the kinetic-energy gain. Thus, the flat band composed of the γ orbital locates higher than E_F even for $\theta = 0$.
- 34) The hopping integrals including the γ orbital are zero in the present model. They are considered to be small in the square-lattice structure in general.
- 35) For instance, we estimate $T_c \lesssim 0.00035t$ at $\theta = 0.139\pi$ by extrapolating the eigenvalues of the Kernel K in eq. (5).
- 36) T. Takeuchi, T. Inoue, K. Sugiyama, D. Aoki, Y. Tokiwa, Y. Haga, K. Kindo and Y. Ōnuki: J. Phys. Soc. Jpn. **70** (2001) 877.
- 37) T. Takeuchi, H. Shishido, S. Ikeda, R. Settai, Y. Haga, and Y. Ōnuki: J. Phys.: Condens. Matter **14** (2002) L261.
- 38) V. F. Correa, L. Tung, S. M. Hollen, P. G. Pagliuso, N. O. Moreno, J. C. Lashley, J. L. Sarrao and A. H. Lacerda: Phys. Rev. B **69** (2004) 174424.
- 39) V. F. Correa, W. E. Okraku, J. B. Betts, A. Migliori, J. L. Sarrao and A. H. Lacerda: Phys. Rev. B **72** (2005) 012407.
- 40) T. Takeuchi: private communication.
- 41) P. Morin and S. J. Williamson: Phys. Rev. B **29** (1984) 1425.